博士学位論文

Study on Toughening Hydrogels through Sacrificial Bonds Formation via Multiple Equilibrium Reactions
（多重平衡反応を利用した犠牲結合形成による ハイドロゲルの強靭化に関する研究）

樫村　尚宏

北海道大学大学院生命科学院

２０２４年９月

Chapter 1: General Introduction

Polymer hydrogels are three-dimensional polymer networks containing large amounts of water, characterized by high water content, low friction, and permeability to substances. The application range of polymer hydrogels has been limited due to their low mechanical properties, which stem from low network density due to water content and various levels of heterogeneity[1]. Over the past 25 years, extensive research has been conducted on improving the mechanical properties of polymer hydrogels, leading to the development of tough polymer hydrogels based on various toughening strategies.

There are two main mechanisms for toughening polymer hydrogels. One is to eliminate the heterogeneity that is considered the source of low mechanical properties. This includes slide-ring gels developed by Ito et al.[2] and Tetra-PEG gels developed by Sakai et al[3]. Slide-ring gels achieve high mechanical properties by introducing dynamic crosslinking points, thereby eliminating heterogeneity originating from crosslinking points. Tetra-PEG gels demonstrate improved mechanical properties by reacting star-shaped polymers with four-branched active terminals to achieve a relatively homogeneous structure.

The other mechanism is the introduction of sacrificial bonds[4]. Sacrificial bonds refer to weak bonds or structures that preferentially break and dissipate energy before the entire material fails. These sacrificial bonds often utilize weak physical interactions such as hydrogen bonds, ionic bonds, hydrophobic interactions, and van der Waals forces[5–10]. Most tough hydrogels enhance their mechanical properties by using physical bonds as sacrificial bonds. A notable example of a special sacrificial bond system is the Double Network gel (DN gel)[11]. DN gels achieve extremely high mechanical properties by utilizing covalent network contrasts in strength and density as sacrificial bonds.

Although the two toughening strategies of structural homogenization and sacrificial bonds differ in their toughening mechanisms, they share the common approach of improving mechanical properties by controlling nanoscale structures and bonds. Thus, regardless of the strategy employed, the relationship between nanoscale structures and bonds and macroscopic mechanical properties is a crucial aspect of polymer hydrogel toughening. This research primarily aims to elucidate the relationship between nanoscale structures and bonds and macroscopic properties in hydrogels with sacrificial bonds.

This dissertation consists of four chapters, with this General Introduction included as Chapter 1.

In Chapter 2, the background of this research is summarized from the aspects of scientific research, including recent studies.

Chapter 3 deals with the toughening of polymer hydrogels by introducing sacrificial bonds, as observed in biological bone tissues.

Reference

(1) Shibayama, M. Spatial Inhomogeneity and Dynamic Fluctuations of Polymer Gels. Macromol. Chem. Phys. 1998, 199. https://doi.org/10.1002/(SICI)1521-3935(19980101)199:1.

(2) Okumura, Y.; Ito, K. The Polyrotaxane Gel: A Topological Gel by Figure-of-Eight Cross-Links. Adv. Mater. 2001, 13 (7), 485–487.

(3) Sakai, T.; Matsunaga, T.; Yamamoto, Y.; Ito, C.; Yoshida, R.; Suzuki, S.; Sasaki, N.; Shibayama, M.; Chung, U. I. Design and Fabrication of a High-Strength Hydrogel with Ideally Homogeneous Network Structure from Tetrahedron-like Macromonomers. Macromolecules 2008, 41 (14), 5379–5384.

(4) Furukawa, H.; Kuwabara, R.; Tanaka, Y.; Kurokawa, T.; Na, Y. H.; Osada, Y.; Gong, J. P. Tear Velocity Dependence of High-Strength Double Network Gels in Comparison with Fast and Slow Relaxation Modes Observed by Scanning Microscopic Light Scattering. Macromolecules 2008, 41 (19), 7173–7178.

(5) Sun, T. L.; Kurokawa, T.; Kuroda, S.; Ihsan, A. B.; Akasaki, T.; Sato, K.; Haque, M. A.; Nakajima, T.; Gong, J. P. Physical Hydrogels Composed of Polyampholytes Demonstrate High Toughness and Viscoelasticity. Nat. Mater. 2013, 12 (10), 932–937.

(6) Zhu, F.; Lin, X. Y.; Wu, Z. L.; Cheng, L.; Yin, J.; Song, Y.; Qian, J.; Zheng, Q. Processing Tough Supramolecular Hydrogels with Tunable Strength of Polyion Complex. Polymer 2016, 95, 9–17.

(7) Haque, M. A.; Kurokawa, T.; Kamita, G.; Gong, J. P. Lamellar Bilayers as Reversible Sacrificial Bonds to Toughen Hydrogel: Hysteresis, Self-Recovery, Fatigue Resistance, and Crack Blunting. Macromolecules 2011, 44 (22), 8916–8924.

(8) Yasui, T.; Zheng, Y.; Nakajima, T.; Kamio, E.; Matsuyama, H.; Gong, J. P. Rate-Independent Self-Healing Double Network Hydrogels Using a Thixotropic Sacrificial Network. Macromolecules 2022, 55 (21), 9547–9557.

(9) Sun, J. Y.; Zhao, X.; Illeperuma, W. R. K.; Chaudhuri, O.; Oh, K. H.; Mooney, D. J.; Vlassak, J. J.; Suo, Z. Highly Stretchable and Tough Hydrogels. Nature 2012, 489 (7414), 133–136.

(10) Liu, C.; Morimoto, N.; Jiang, L.; Kawahara, S.; Noritomi, T.; Yokoyama, H.; Mayumi, K.; Ito, K. Tough Hydrogels with Rapid Self-Reinforcement. Science 2021, 372 (6546), 1078–1081.

(11) Gong, J. P.; Katsuyama, Y.; Kurokawa, T.; Osada, Y. Double-Network Hydrogels with Extremely High Mechanical Strength. Adv. Mater. 2003, 15 (14), 1155–1158.

Chapter 2: Background

2-1: Sacrificial bond

Sacrificial bonds are weak bonds or structures that break and dissipate energy prior to the failure of the entire material. This concept was first proposed by Nacre, suggesting that interactions between biological polymers and biological minerals act as sacrificial bonds[1]. The concept has expanded to other biological tissues, explaining the mechanical properties of many tough biological tissues such as bone and spider silk. Particularly after the proposal of sacrificial bonds in bone tissue in 2001[2,3], numerous studies on bone sacrificial bonds have been conducted to this day[2,4–6]. Details will be discussed in Chapter 3.

Until the late 2000s, this concept was primarily associated with biological tissues. In 2008, Gong et al. first incorporated it as a toughening principle for artificial materials, resulting in DN gels[7]. Typical DN gels consist of a hard and brittle first network and a soft and stretchable second network[8]. During deformation, the covalent bonds of the hard and brittle first network preferentially break[9]. While ordinary gels would fail at this point, DN gels avoid overall material failure due to the presence of the second network. As a result, additional energy is required to break the first network to cause overall DN gel failure, making the material as a whole tougher[10].

This concept of sacrificial bonds in polymer network materials has become widespread, leading to the development of various tough materials with sacrificial bonds[11–20]. Materials using physical bonds as sacrificial bonds have been extensively developed as self-healing tough materials due to their ability to rebond after breakage[20]. Recent attention has focused on strain-induced crystallization gels and elastomers, whose toughness originates from strain-induced crystals acting as sacrificial bonds, making them a type of sacrificial bond material[21–23].

While sacrificial bonds were originally a concept explaining the toughness of biological tissues, they are now well-known as a toughening strategy for polymer network materials such as gels and elastomers. Consequently, much is understood about sacrificial bonds in polymer network materials, while understanding the mechanisms in biological tissues remains limited due to their complexity. Chapter 3 aims to bridge this gap between artificial materials and biological tissues by reproducing the sacrificial bonds of biological tissues, particularly bone tissue, in artificial materials.

2-2:

Reference

(1) Wang, R.; Gupta, H. S. Deformation and Fracture Mechanisms of Bone and Nacre. *Annu Rev Mater Res* **2011**, *41*, 41–73. https://doi.org/10.1146/annurev-matsci-062910-095806.

(2) Currey, J. Sacrificial Bonds Heal Bone. *Nature* **2001**, *414* (6865), 699. https://doi.org/10.1038/414699a.

(3) Thompson, J. B.; Kindt, J. H.; Drake, B.; Hansma, H. G.; Morse, D. E.; Hansma, P. K. Bone Indentation Recovery Time Correlates with Bond Reforming Time. *Nature* **2001**, *414* (6865), 773–776. https://doi.org/10.1038/414773a.

(4) Fantner, G. E.; Hassenkam, T.; Kindt, J. H.; Weaver, J. C.; Birkedal, H.; Pechenik, L.; Cutroni, J. A.; Cidade, G. A. G.; Stucky, G. D.; Morse, D. E.; Hansma, P. K. Sacrificial Bonds and Hidden Length Dissipate Energy as Mineralized Fibrils Separate during Bone Fracture. **2005**. https://doi.org/10.1038/nmat1428.

(5) Fantner, G. E.; Hassenkam, T.; Kindt, J. H.; Weaver, J. C.; Birkedal, H.; Pechenik, L.; Cutroni, J. A.; Cidade, G. A. G.; Stucky, G. D.; Morse, D. E.; Hansma, P. K. Sacrificial Bonds and Hidden Length Dissipate Energy as Mineralized Fibrils Separate during Bone Fracture. *Nat Mater* **2005**, *4* (8), 612–616. https://doi.org/10.1038/nmat1428.

(6) Lieou, C. K. C.; Elbanna, A. E.; Carlson, J. M. Sacrificial Bonds and Hidden Length in Biomaterials: A Kinetic Constitutive Description of Strength and Toughness in Bone. *Phys Rev E Stat Nonlin Soft Matter Phys* **2013**, *88* (1), 1–10. https://doi.org/10.1103/PhysRevE.88.012703.

(7) Furukawa, H.; Kuwabara, R.; Tanaka, Y.; Kurokawa, T.; Na, Y. H.; Osada, Y.; Gong, J. P. Tear Velocity Dependence of High-Strength Double Network Gels in Comparison with Fast and Slow Relaxation Modes Observed by Scanning Microscopic Light Scattering. *Macromolecules* **2008**, *41* (19), 7173–7178. https://doi.org/10.1021/MA800821J/ASSET/IMAGES/LARGE/MA-2008-00821J_0009.JPEG.

(8) Gong, J. P.; Katsuyama, Y.; Kurokawa, T.; Osada, Y. Double-Network Hydrogels with Extremely High Mechanical Strength. *Advanced Materials* **2003**, *15* (14), 1155–1158. https://doi.org/10.1002/adma.200304907.

(9) Matsuda, T.; Kawakami, R.; Namba, R.; Nakajima, T.; Gong, J. P. Mechanoresponsive Self-Growing Hydrogels Inspired by Muscle Training. *Science (1979)* **2019**, *363* (6426), 504–508. https://doi.org/10.1126/science.aau9533.

(10) Gong, J. P. Why Are Double Network Hydrogels so Tough? *Soft Matter* **2010**, *6* (12), 2583–2590. https://doi.org/10.1039/b924290b.

(11) Fukao, K.; Nonoyama, T.; Gong, J. P.; Tanaka, K.; Kiyama, R. Hydrogels Toughened by Biominerals Providing Energy-Dissipative Sacrificial Bonds. *J Mater Chem B* **2020**, *8* (24), 5184–5188. https://doi.org/10.1039/d0tb00833h.

(12) Haque, M. A.; Kurokawa, T.; Kamita, G.; Gong, J. P. Lamellar Bilayers as Reversible Sacrificial Bonds to Toughen Hydrogel: Hysteresis, Self-Recovery, Fatigue Resistance, and Crack Blunting. *Macromolecules* **2011**, *44* (22), 8916–8924. https://doi.org/10.1021/ma201653t.

(13) Takahashi, R.; Sun, T. L.; Saruwatari, Y.; Kurokawa, T.; King, D. R.; Gong, J. P. Creating Stiff, Tough, and Functional Hydrogel Composites with Low-Melting-Point Alloys. *Advanced Materials* **2018**, *30* (16), 1–7. https://doi.org/10.1002/adma.201706885.

(14) Luo, F.; Sun, T. L.; Nakajima, T.; Kurokawa, T.; Zhao, Y.; Sato, K.; Ihsan, A. Bin; Li, X.; Guo, H.; Gong, J. P. Oppositely Charged Polyelectrolytes Form Tough, Self-Healing, and Rebuildable Hydrogels. *Advanced Materials* **2015**, *27* (17), 2722–2727. https://doi.org/10.1002/adma.201500140.

(15) Gaharwar, A. K.; Dammu, S. A.; Canter, J. M.; Wu, C. J.; Schmidt, G. Highly Extensible, Tough, and Elastomeric Nanocomposite Hydrogels from Poly(Ethylene Glycol) and Hydroxyapatite Nanoparticles. *Biomacromolecules* **2011**, *12* (5), 1641–1650. https://doi.org/10.1021/bm200027z.

(16) Sun, J. Y.; Zhao, X.; Illeperuma, W. R. K.; Chaudhuri, O.; Oh, K. H.; Mooney, D. J.; Vlassak, J. J.; Suo, Z. Highly Stretchable and Tough Hydrogels. *Nature* **2012**, *489* (7414), 133–136. https://doi.org/10.1038/nature11409.

(17) Liu, R.; Liang, S.; Tang, X. Z.; Yan, D.; Li, X.; Yu, Z. Z. Tough and Highly Stretchable Graphene Oxide/Polyacrylamide Nanocomposite Hydrogels. *J Mater Chem* **2012**, *22* (28), 14160–14167. https://doi.org/10.1039/c2jm32541a.

(18) Zhang, H. J.; Sun, T. L.; Zhang, A. K.; Ikura, Y.; Nakajima, T.; Nonoyama, T.; Kurokawa, T.; Ito, O.; Ishitobi, H.; Gong, J. P. Tough Physical Double-Network Hydrogels Based on Amphiphilic Triblock Copolymers. *Advanced Materials* **2016**, *28* (24), 4884–4890. https://doi.org/10.1002/adma.201600466.

(19) Luo, F.; Sun, T. L.; Nakajima, T.; King, D. R.; Kurokawa, T.; Zhao, Y.; Ihsan, A. Bin; Li, X.; Guo, H.; Gong, J. P. Strong and Tough Polyion-Complex Hydrogels from Oppositely Charged Polyelectrolytes: A Comparative Study with Polyampholyte Hydrogels. *Macromolecules* **2016**, *49* (7), 2750–2760. https://doi.org/10.1021/acs.macromol.6b00235.

(20) Sun, T. L.; Kurokawa, T.; Kuroda, S.; Ihsan, A. Bin; Akasaki, T.; Sato, K.; Haque, M. A.; Nakajima, T.; Gong, J. P. Physical Hydrogels Composed of Polyampholytes Demonstrate High Toughness and Viscoelasticity. *Nat Mater* **2013**, *12* (10), 932–937. https://doi.org/10.1038/nmat3713.

(21) Hashimoto, K.; Enoki, T.; Liu, C.; Li, X.; Sakai, T.; Mayumi, K. Strain-Induced Crystallization in Tetra-Branched Poly(Ethylene Glycol) Hydrogels with a Common Network Structure. *Macromolecules* **2024**. https://doi.org/10.1021/ACS.MACROMOL.3C02038.

(22) Fujiyabu, T.; Sakumichi, N.; Katashima, T.; Liu, C.; Mayumi, K.; Chung, U. Il; Sakai, T. Tri-Branched Gels: Rubbery Materials with the Lowest Branching Factor Approach the Ideal Elastic Limit. *Sci Adv* **2022**, *8* (14), 10. https://doi.org/10.1126/SCIADV.ABK0010.

(23) Liu, C.; Morimoto, N.; Jiang, L.; Kawahara, S.; Noritomi, T.; Yokoyama, H.; Mayumi, K.; Ito, K. Tough Hydrogels with Rapid Self-Reinforcement. *Science (1979)* **2021**, *372* (6546), 1078–1081. https://doi.org/10.1126/SCIENCE.AAZ6694.

Chapter 3: Synthesis of tough hydrogel with bone like sacrificial bond

3-1 Introduction

Learning from nature is a promising approach to achieve high functionality of synthetic materials[1–3]. One of the decisive differences between living tissues and man-made materials is their self-regulation function during the metabolic process[4,5]. In nature, not only soft but also hard tissues grow, repair, and optimize themselves through repeated degradation and regeneration[6–8]. Among them, bone is a typical hard and active tissue with biochemical and biomechanical functionalities, remodeled by the harmonization of osteoblasts and osteoclasts[7,8]. In the bone formation by osteoblasts, they simply secrete macromolecular building components and enzymes to provide an environment for the spontaneous occurrence of biomineralization from body fluid[9–11]. Namely, the bone formation is a chemical event outside the cells[9]. The major molecular components of bone are low crystalline hydroxyapatite (HAp), type I collagen, non-collagenous proteins (NCP), proteoglycans, and a small amount of water [12–14]. HAp, which is an inorganic mineral of calcium phosphate located in gaps of collagen fibrils, acts as a storage/supplier of calcium and phosphate ions. NCPs such as osteopontin (OPN) and osteocalcin, which are rich in acidic residues, intercalate into the mineralized collagen fibril interfaces through calcium ions[15]. OPN has about 300 residues and contains many acidic amino acids such as glutamic acid and aspartic acid[16,17]. Considering those of phosphorylation by post-translational modifications, the OPN has about 39% of acidic residues at most [18]. OPNs forms a glue-like network through calcium-mediated ionic bonding with the acidic residues. The glue-like network adheres to the mineralized collagen fibrils through calcium mediated bonding between carboxyl group of OPNs and minerals complexed with collagen fibrils. According to the past investigations by using atomic force microscopy [15,18,19], genetic modification techniques [20], and molecular simulations [21–23], the molecular origin of high toughness of bone is that the ionic bonds formed in the self-regulation are preferentially ruptured under impact and deformation (**Figure 3-1A**). The preferential rupture of relatively weak bonds suppresses the local stress concentration and dissipates energy, preventing macroscopic catastrophic fracture (e.g. bone fracture). Thus, such weak bond has been called “sacrificial bond”[19,24] as an intrinsic molecular mechanism for toughening of bones. Moreover, accompanying with the dissociation of ionic bonds, it has been suggested that the covalent crosslinking structures of both intra and inter molecules of OPN enhance energy dissipative capability [16]. The OPN is enzymatically operated by transglutaminase II (TG), resulting covalent crosslinking of glutamine and lysine residues in OPN [25]. The result suggests that the covalent crosslinking promotes the effect of sacrificial bonds.

Inspired from the molecular structure of the bone and its chemical characteristics, here, we propose a novel strategy to develop tough hydrogels utilizing a series of coupled chemical equilibriums, adopting polyacrylic acid (PAAc) as weak acidic polymers to mimic OPN and HAp particles as self-regulating calcium ion source for sacrificial ion bonds formation in the hydrogels (**Figure 3-1B**). The hydrogels can be synthesized from AAc monomers in the presence of chemical crosslinker and HAp particles and then equilibrated in pure water

(**Figure 3-1C**). In such a system, five equilibrium reactions (**Figure 3-2A, B**) are coupled to regulate the ionic bond formation between polymers and between polymer and minerals. The generation of H^+ by dissociation of -COOH on PAAc (reaction 1) triggers the dissolution of HAp (reaction 2), releasing calcium ions Ca^{2+} and phosphate ions PO_4^{3+}; the released PO_4^{3+} ions act as buffer to keep the concentration of H^+ constant (reaction 3); the released Ca^{2+} ions form ionic bonds with $-COO^-$ groups of PAAc (reaction 4) and the Ca^{2+} ions on HAp surface form ionic bonds with $-COO^-$ of PAAc (reaction 5), both further promote the dissociation of the carboxyl groups (reaction 1). When all of the $-COO^-$ groups are bound to Ca^{2+} ions, the increase of free Ca^{2+} ion concentration suppresses further dissolution of HAp. As a result, formation of inter and intra-chain ionic bonds between Ca^{2+} ions and $-COO^-$ on PAAc and the adsorption of PAAc on the solid phase HAp are self-regulated by these five coupled reactions. Thus, the HAp particles function as reservoirs to automatically supply the optimized amount of Ca^{2+} ions to form ionic bonds in the PAAc hydrogels.

Such bone-like self-regulative mechanism makes the PAAc/HAp system unique, in difference from common organic/inorganic composites consist of polymers and chemically inert inorganic particles[26–29]. In the common composites, the inorganic articles only serve as hard fillers, and they do not facilitate the dynamic bonds formation of the soft matrix. Moreover, the PAAc/HAp system is different from common ionic bonds-based tough hydrogels, such as polyampholyte hydrogels or polyion complex hydrogels. In these hydrogels, the charge balance should be strictly pre-controlled in preparation state otherwise the hydrogels would significantly swell by the polyelectrolyte effect and destroy the ionic bonds[30,31], while the PAAc/HAp system is able to optimize its structure to reach the maximum amount of ionic bonds by the self-regulating mechanism. Accordingly, this bone-inspired self-regulatory mechanism provides a novel promising approach to create tough composites with optimized structure.

3-2 Methods

Materials

Acrylic acid (AAc), *N, N'*-methylenebisacrylamide (MBAA), potassium persulfate (KPS), Methacrylic acid (MAc), 2-oxoglutalic acid and liquid paraffin (paraffin oil) were purchased from Wako Pure Chemical Industries, Ltd. (Japan) and used as received. Hydroxyapatite particles and sodium acrylate (NaAc) were purchased by Sigma-Aldrich Inc. (U.S.A.) and used as received. Acrylamide (AAm) was purchased from Junsei Chemical Co. Ltd. (Japan) and used as received. Ethanol denatured with about 4% isopropanol was purchased from Imazu Chemical Co., Ltd. (Japan) and used as received. HAp particles (cumulant diameter of c. a. 1 μm, polydispersity index, PI: 2.5, **Figure 3-1C**) was purchased from Sigma Aldrich and used as received. HAp disc plate (1 mm thickness, 32 mm diameter) was purchased from NGK SPARK PLUG Co., Ltd. and used after washing by 10% ethanol solution.

Preparation of PAAc/HAp Gels

Briefly, PAAc/HAp gels were obtained by one-step thermal radical polymerization of HAp particles suspended aqueous solution containing acrylic acid, cross-linking agent, and thermal initiator (**Figure 3-1C**).

In specific, prescribed amount of AAc monomer, MBAA cross-linker, and KPS thermal initiator were dissolved in pure water. Then a precursor slurry was obtained by adding prescribed amount of HAp particles to the solution. The slurry was mixed with removing bubbles by vacuum rotation/revolution mixer (ARV-310LED, THINKY, Japan) at 300 kPa, 300 rpm for 3 min. The slurry was poured into a reaction cell and sealed. The reaction cell was composed of a pair of glass plates separated by a silicone spacer of 2 mm-thick. The reaction cell was immersed in a warm water bath of 65 °C to conduct polymerization for 12 h. The concentration of AAc was varied from 1 to 3 M, and the concentration of MBAA was varied from 0.025 to 3 mol% (referred to AAc), and the concentration of KPS was kept at 0.1 mol% (referred to AAc). HAp was varied from 5 to 15 vol% (referred to total volume of the suspension). The pristine PAAc gel without HAp particles as a reference sample was obtained in the same way. The PMAc/HAp gel was prepared by using MAc as monomer instead of AAc.

Swelling and Deswelling of Gels in Water

The as-prepared PAAc/HAp gels and PAAc gels of 2 mm-thick were cut into discs and immersed in pure water. The water was changed daily and the thickness (t) was measured with a thickness gauge each time. The swelling volume ratio (V/V_0) was calculated from the following relation with the initial thickness (t_0) because of isotropic swelling of the gels.

$$\frac{V}{V_0} = \left(\frac{t}{t_0}\right)^3$$

Attenuated Total Reflectance Fourier Transform Infrared Spectroscopy (ATR-FTIR)

ATR-FTIR spectroscopy was carried out with FT/IR-6600 spectrometer (JASCO, Japan). The surface of gel was gently wiped to remove the surface excess water and then was contacted to the ATR diamond prism. Measurements were conducted with 64 integrations, resolution of 2 cm^{-1}, and wavenumber range of 1900-1300 cm^{-1}.

The complexation degree α of the carboxyl group of PAAc with HAp is determined from the peak areas at 1550 cm^{-1} (assigned to COO^-) and 1700 cm^{-1} (assigned to COOH) [32], using the following relation,

$$\alpha = \frac{c_{COO^-}}{c_{COOH} + c_{COO^-}} = \frac{\frac{A_{1550}}{A_{1700}}}{\frac{\varepsilon_{1550}}{\varepsilon_{1700}} + \frac{A_{1550}}{A_{1700}}} = \frac{\frac{A_{1550}}{A_{1700}}}{2.726 + \frac{A_{1550}}{A_{1700}}}$$

where c, A and ε were concentration of each moiety, area of IR spectral peak, and molar absorption coefficient, respectively. To estimate peak areas at 1550 and 1700 cm^{-1}, the spectral profile of sample was firstly subtracted by the pure water's profile. Then, these peaks were curve-fitted by pseudo-Voigt function. Each area was calculated from the integral of de-convoluted peak. A calibration curve was generated from measurements of 1 M poly(NaAc-*co*-AAc) gels with various copolymerization ratios to determine the molar absorption coefficient of the peaks at 1550 cm^{-1} and 1700 cm^{-1} (**Figure 3-S1**). Their ratio $\varepsilon_{1550}/\varepsilon_{1700}$ was determined to 2.73.

Thermogravimetry and Differential Thermal Analysis (TG-DTA)

Thermogravimetry and Differential Thermal Analysis (TG-DTA) was performed by Thermo plus EVO II TG8120 HUM-1F. Approximately 20 mg of PAAc/HAp gel was cut out and heated up to 700°C at a rate of 5°C/min to evaporate the water and burn off the polymeric component to obtain the results.

Inductively Coupled Plasma Atomic Emission Spectroscopy (ICP-AES)

Inductively coupled plasma atomic emission spectroscopy (ICP-AES) was performed on an ICP-AES spectrometer ICPE-9000 (Shimadzu Corporation, Japan). A disc (2 mm of thickness, 1 mm of diameter) of as-prepared PAAc/HAp gel (composition: 3M AAc, 1 mol % MBAA, 0.1 mol % KPS, 10 vol % HAp) was immersed in 200 mL pure water, and the water was periodically changed with the fresh water. Each immersed water was collected for ICP-AES analysis to determine calcium and phosphorus diffused out from the PAAc/HAp gel (**Figure 3-S4**).

Uniaxial Tensile Test

Uniaxial tensile tests were performed by using a tensile-compressive tester (Instron 5965 type universal testing system, Instron co., US). The gels equilibrated in pure water were cut into dumbbell-shape of international standard dimension ISO 37-2 (12 mm in length, 2 mm in width) using a mechanical cutting machine. The test was done in 100 mm/min velocity at room temperature. Work of extension was calculated from the integral area under the stress-strain curve to the point of fracture. The cyclic loading/unloading test was performed to evaluate the dissipated energy and healing ratio. The gel sample was deformed up to strain $\varepsilon = 2$. The dissipated energy was comparable to the hysteresis area U_{hys} as follows,

$$U_{hys} = \int_0^2 \left(\sigma_{load}(\varepsilon) - \sigma_{unload}(\varepsilon)\right) d\varepsilon$$

Where $\sigma_{load}(\varepsilon)$ and $\sigma_{unload}(\varepsilon)$ were the loading and unloading stress, respectively. For recovering evaluation, the intervals between 1st and 2nd cycles were 0, 1, 10, 60 and 1440 min. During the testing, the samples were covered with paraffin oil to prevent drying. The healing ratio was calculated from U_{hys} of the 1st cycle over that of 2nd cycle.

Peeling test

A 90° peel test was performed to evaluate the adhesion of PAAc gels to HAp plate. The PAAc gels were polymerized on HAp plate and the measurement was performed for the as-prepared sample without swelling in water. Polyacrylamide (PAAm) gel was prepared as a control gel without acid residues. The PAAc gel and the PAAm gel were polymerized by photosynthesis using 2-oxoglutalic acid as a photoinitiator. The concentration of monomer (AAc or AAm) was 4 M, the concentration of MBAA was 0.01 mol%, and the concentration of 2-oxoglutalic acid was 0.01 mol%. To prevent elongation of the cramped handles the gels were supported with a tape over the cramped handles. The handle was pulled at a speed of 100 mm/min by a universal tensile tester (tensilon). Adhesion energy was calculated from the area of force extension curve.

3-3 Results and Discussion

Self-regulated complexation via calcium mediated ionic bonds in PAAc/HAp hydrogels

Figure 3A showed the appearance of as-prepared PAAc/HAp gel and its equilibrium state in pure water. The gel was prepared from 3 M AAc, 0.1 mol% MBAA, and 10 vol% HAp. As a typical example, the as-prepared gel was opaque due to the presence of HAp micro-particles, and the gel volume decreased at equilibrium state in pure water by a fact of 0.6~0.7 in relative to its as-prepared state, indicating the formation of ionic bonds. The chronological detail in volume change was measured with the comparison to that of pristine PAAc gel with the absence of HAp particles (**Figure 3-3B**). The pristine PAAc gel showed simple swelling behavior in similar to general polyelectrolyte gels. On the other hand, the PAAc/HAp gel showed a unique non-monotonous volume change. Initially, the gel exhibited swelling in water. After ~1000 min, the gel shrank and finally lost about one third of its original volume at equilibrium. This implies that the calcium-mediated ionic bonds were gradually formed inside the gel by the self-regulative equilibriums.

To identify the dissociation of COOH group on PAAc (reaction 1), attenuated total reflection Fourier transform infrared (ATR-FTIR) spectroscopy was performed on the PAAc/HAp gel and the pristine PAAc gel adjusted to the same volume of the swelling equilibrium PAAc/HAp gel (**Figure 3-3C**). The PAAc gel mainly showed a strong peak at 1700 cm^{-1} assigned to C=O stretching vibration of COOH and a weak one around 1550 cm^{-1} assigned to the stretching vibration of inverse-paired COO^-, meaning that PAAc moieties did not de-protonate so much. Similar to the PAAc gel, the as-prepared PAAc/HAp gel also had the small peak around 1550 cm^{-1}, while the peak at equilibrium in pure water was strongly enhanced. This peak enhancement indicates that the carboxyl group was deprotonated and the formation of ionic bond between COO^- and calcium ion (reaction 4) was promoted during the immersion in water. To confirm the coupling between the reactions shown in **Figure 3-2A**, the relation between volume change and formation of calcium-mediated ionic bond was chronologically evaluated (**Figure 3-3D**). The complexation degree (α) was calculated from ratio of the IR peak integral of COO^- and sum of COO^- and COOH. In the initial period (~60 min), the swelling was still mild, and the α was almost constant around 0.1. After that, as swelling proceeded, the α simultaneously increased, suggesting that immersion in water leads to the dissociation and swelling is induced by the osmotic pressure generated by dissociated proton ions. The swelling reached a maximum around α=0.3 and then shrinking occurred with time. However, the α kept increasing even the PAAc/HAp gel became shrinking, and finally equilibrated to ~0.45. This delayed shrinkage behavior indicates that the HAp dissolved to generate Ca^{2+} ions (reaction 2) by proton generation, leading to ionic bond formation. The shrinkage behavior was generally observed in other compositions, including HAp concentration, AAc concentration, (**Figure 3-S2**). For almost all of these gels, approximately 40~60% of carboxyl groups were dissociated and form ionic bonds with calcium ions in these systems. Furthermore, we also observed the shrinkage of the PMAc/HAp gel, in which methacrylic acid (MAc) was used as monomer instead of AAc (**Figure 3-S2**).

To verify the ionic bond formation by the coupled reactions during the self-regulation, we investigated the polymer/mineral weight ratio of equilibrate PAAc/HAp gel calculated from

thermogravimetry and differential thermal analysis (TG-DTA). We found that the ratio was 0.72 for PAAc/HAp gel of formulation 3 M AAc, 0.1 mol% MBAA, and 10 vol% HAp (**Figure 3-S3**), which is higher than the feed polymer/mineral weight ratio of 0.68 in the preparation. This indicates the dissolution of HAp and release from the PAAc/HAp gel immersed in water. Measurement of calcium and phosphorus atoms released from the PAAc/HAp gel by inductively coupled plasma atomic emission spectroscopy (ICP-AES) showed that approximately 11% calcium (0.33 M) and 37% phosphorus (0.67 M) atoms in relative to the initial total amount were released from the gel (**Figure 3-S4**). This suggests that at least 37% of HAp was dissolved, assuming that the dissolved phosphate ions were all diffused into solutions. Therefore, at least 26% of calcium atoms (of 0.78 M) remain in the PAAc/HAp gel, in ionic state. The 0.78 M calcium ions is very close to half of the concentration of dissociated carboxylic groups 1.68 M (56% of 3 M). This confirms that the dissociated carboxylic groups almost fully formed ionic bonds with the calcium ions. Thus, the number of net charges in the gels are spontaneously regulated to zero through these coupled reactions in which the HAp micro-particles act as calcium ion reservoirs. The ion concentrations in the gel and in the solution are summarized in **Table 3-1**.

As shown in **Figure 3-2B**; two types of the calcium-mediated ionic bond should exist in this system: one is the cross-linking of intra/inter PAAc strands by divalent calcium ions provided by HAp, and the other is the bond between PAAc and calcium ions at the outermost surface of HAp particles (33, 34). The valence of ionized calcium at the outermost surface of HAp is considered to be monovalent. The bonding of PAAc network to HAp was further confirmed by the debonding test of a pristine PAAc hydrogel prepared on a bulk HAp plate (**Figure S5**). The adhesion strength of the as-prepared PAAc gel on HAp was 10 times of a non-acidic polyacrylamide gel network, confirming the calcium-mediated ionic bonding between PAAc gel and HAp, as-like the interaction between OPN and HAp. We consider that the number of carboxylic groups in bonding to the HAp is much less than those in binding to the divalent calcium ions, and is not included in the rough estimation shown in **Table 3-1**.

From these results, the swelling and subsequent shrinking of PAAc/HAp gel can be explained as **Figure 3E**. The swelling of a polyelectrolyte gel is influenced by three factors: osmotic pressure Π_{mix} contributed by the polymer, elastic pressure Π_{el} due to the deformation of the gel network, and osmotic pressure Π_{ion} due to the concentration difference of small ions between the inside and outside of the gel. When the as-prepared PAAc/HAp gel is immersed in pure water, the $\Pi_{ion}$is large in the earliest stage because of the proton ions deprotonated from the PAAc. Taking the Π_{mix} and Π_{ion} as the driving force, the gel shows swelling in the early period. During the immersion, calcium ions dissolved from HAp and those on the surface of HAp are exchanged with proton of carboxyl side chains and form ionic bond with COO^- which serves as cross-linking, and the exchanged proton form pair with phosphorus ions dissolved from HAp and diffuse out from PAAc/HAp gel. The additional cross-linking by ionic bond formation contributes to the increase of Π_{el} and the diffusion of protons and phosphorus ions from the gels decreases the mobile ion concentration difference between inside and outside of the gel, contributing to the decrease of Π_{ion}. Both effects favor shrinking. As a result, the gel first swells and then shrinks with time due to coupled reactions.

Toughening by sacrificial bonds

To evaluate the effect of self-regulated sacrificial bonds on the toughening of gels, uniaxial tensile tests and loading-unloading tests were conducted. As a typical example, the results for the formulation of 3M AAc, 0.1 mol % MBAA, 10 vol % HAp is shown in **Figure 3-4**. As a control sample, we prepared pure PAAc gel whose swelling ratio was adjusted to the same that of PAAc/HAp gel equilibrated in pure water ($V/V_0 \sim 0.65$). The equilibrium-swollen pure PAAc gel broke at very low strain and stress, while the equilibrium-swollen PAAc/HAp gel showed significant improvement in both fracture stress and strain (**Figure 3-4A**). The high breaking strain was comparable to that of the adjusted PAAc gel, implying that the gel shrinkage primarily contributes to the high elongation in the PAAc/HAp gel, which can be interpreted as the spontaneous folding of the gel network strands via self-regulation process. Since the ionic bond is obviously weaker than the covalent bond, the ionic cross-link structure was preferentially fractured by deformation to dissipate energy. The opening of ionic bonds lengthens the network strand length and provides the polymer network an extra stretching capacity. This phenomenon is known as "hidden length" effect, observed in bones and materials possessing sacrificial bond [15,33]. Next, the loading-unloading test up to strain 2.0 was performed to observe mechanical hysteresis, corresponding to the energy dissipation by sacrificial bonds (**Figure 3-4B**). The swelling adjusted PAAc gel showed almost no hysteresis (3.36 kJ/m^3), meaning that the gel network structure was not fractured at all and there is no sacrificial bonds. The as-prepared PAAc/HAp gel showed obvious hysteresis (48.5 kJ/m^3), and it was enhanced after equilibrium in pure water (161 kJ/m^3), agreeing with the increment of complexation degree α.

The calcium-mediated ionic bonds are physical bonds that potentially reform even after breakage. **Figure 3-4C** and **3-4D** shows the cyclic tests with different waiting times and healing ratio calculated from the hysteresis ratio of each waiting time and the 1st cycle. The hysteresis was recovered to ~75% at most within 24 hours, indicating that the major energy dissipation term is the calcium-mediated ionic bond. The incomplete recovery would be due to the rapture of the chemical cross-linker as irreversible covalent bond.

Effect of covalent cross-linking structure in the sacrificial bond system

As mentioned in **Figure 3-1A**, the OPN has both calcium mediated ionic bond and covalent cross-link structure. It is considered that they synergistically contribute to the toughness of bone structure. A quantitative study of the effect of covalent cross-linker in OPN has not been reported yet because evaluation of the density of covalent cross-link points is challenging. Here, we systematically tuned the covalent cross-link structure of PAAc/HAp gel by changing the concentration of chemical cross-linker MBAA during polymerization of PAAc. **Figure 3-5** shows a series of PAAc/HAp gels with different MBAA cross-linker concentrations from 0.025 to 3 mol% in relative to AAc monomer concentration, and 3 M AAc and 10 vol% HAp were used. When these gels were immersed in pure water, all gels showed shrinking to the similar volume at equilibrium (**Figure 3-5A**). However, swelling-shrinking self-regulation process differed depending on the cross-linker concentration. The gels with low cross-linker concentrations exhibited high transient swelling peak up to 10 folds of their original volumes. The gels with high cross-linker concentrations showed shrinking without initial swelling. This should be due to an increase in elastic pressure, which

exceeded the osmotic pressure even in the initial period. However, the transient swelling, which results in temporal decrement of polymer and HAp concentrations, did not affect the final equilibrium volume. **Figure 3-5B** shows the degree of complexation α of as-prepared and equilibrated gels with various cross-linker concentrations. The α at both initial and equilibrated states was almost constant against the cross-linker concentration. These results suggest that the density of cross-link structure has no effect on the formation of calcium-mediated ionic bond and the final volume. **Figure 3-5C** showed tensile stress-strain curves of PAAc/HAp gels with different cross-linker concentrations. The Young's modulus was summarized with those of as-prepared gels in **Figure 3-5D**. In the low concentration of cross-linker, the modulus was greatly increased after equilibrium, meaning that the calcium mediated ionic bond is the major contribution on the gel modulus. When the cross-linker concentration was increased, the modulus gap between as-prepared and equilibrated states decreased. As shown in **Figure 3-5B**, the complexation degree was almost the same in all cross-linker concentrations. Therefore, even though the calcium mediated ionic cross-link structure was formed, the contribution was relatively small in the total cross-link density. The similar tendency was observed in the hysteresis (**Figure 3-5E and 3-5F**). Takahashi et al. suggest that high matrix modulus enhances efficient energy dissipation via sacrificial macroscopic structure inspired by hydrogel sacrificial bonds [34]. Therefore, the large hysteresis in samples with high cross-linker concentration indicates the efficient energy dissipation due to high modulus of PAAc gel matrix. As shown in **Figure 3-5G**, the fracture strain and the work of extension increased with increasing in cross-linker concentration and reached a maximum around 0.1 mol% MBAA. The trend above 0.1 mol%, that is, increasing in cross-linker concentration results in the decreasing of the fracture strain and the work of extension, is consistent with common network materials due to decrease in the network strand length of the non-covalent network The opposite trend observed below 0.1 mol%, suggests that a different fracture mechanism was working. From the results of the Young's modulus (**Figure 3-5G**) and the hysteresis (**Figure 3-5F**), calcium mediated cross-link structure was the main contribution for the gel structure instead of the covalent cross-link in this low MBAA region (**Figure 3-5H**). Therefore, the calcium-mediated cross-link structure effectively served as sacrificial bonds to govern the fracture of the gels. It is interesting to see that the fracture strain and work of extension to fracture increased with (**Figure 3-5G**) while the modulus decreased with (**Figure 3-5D**) the increase of MBAA concentration in this region. Since the swelling ratio and the degree of complexation α of the equilibrated gels hardly changed with MBAA concentrations, the decreasing trend of the Young's modulus is probably due to dynamic effect of the ionic bond that becomes less stable at high MBAA concentration. Along this line the increasing trend of fracture strain and work of extension could also be understood by such dynamic effect. That is, when the dynamic bond is too stable at the observation time scale, the fracture strain might decreases. These results suggest the interplay of covalent cross-link and the dynamic sacrificial bonds, and the structure of this system is optimized at 0.1 mol% MBAA for the sacrificial bond to work. This result gives insight on the synergistic effects of calcium mediated ionic bond and covalent cross-link structure of OPN in bone[16].

3-4 Conclusion

Formation of the calcium mediated ionic bonds as sacrificial bonds is self-regulated by coupling of multiple equilibrium reactions in a system consists of PAAc network and HAp nano particles, which effectively toughens the synthetic hydrogels with various compositions. There is an optimum chemical cross-linker concentration of the polymer network to maximize the effect of the calcium mediated ionic bonds as sacrificial bonds. This system is designed based on our assumption that the process of sacrificial bond formation in bone has a self-regulatory mechanism in which HAp and OPN play critical roles. Although the sacrificial bond mechanism for bone toughness was proposed over 20 years ago[19,24] and it has inspired many artificial sacrificial bond materials[35–39], few have focused on the mechanism of sacrificial bond formation in the body, because of their complexity. Our artificial approach enables us to evaluate the relationship between self-regulated sacrificial bond formation mechanism in molecular scale and mechanical strength and toughness in macroscopic materials, which gives deep insight on the mechanism of sacrificial bond formation for high toughness of bones. We postulate that the self-regulation mechanism makes bone self-adaptive to the environment changes. Such a self-regulation mechanism is considered the reason that why the nature choose HAp as the inorganic component for bones and hard tissues.

REFERENCES

(1) du Plessis, A.; Broeckhoven, C.; Yadroitsava, I.; Yadroitsev, I.; Hands, C. H.; Kunju, R.; Bhate, D. Beautiful and Functional: A Review of Biomimetic Design in Additive Manufacturing. Addit Manuf 2019, 27, 408–427. https://doi.org/10.1016/J.ADDMA.2019.03.033.

(2) Wegst, U. G. K.; Bai, H.; Saiz, E.; Tomsia, A. P.; Ritchie, R. O. Bioinspired Structural Materials. Nat Mater 2015, 14 (1), 23–36. https://doi.org/10.1038/nmat4089.

(3) Su, B.; Tian, Y.; Jiang, L. Bioinspired Interfaces with Superwettability: From Materials to Chemistry. J Am Chem Soc 2016, 138 (6), 1727–1748. https://doi.org/10.1021/JACS.5B12728/ASSET/IMAGES/LARGE/JA-2015-12728R_0025.JPEG.

(4) Slominski, A.; Wortsman, J. Neuroendocrinology of the Skin. Endocr Rev 2000, 21 (5), 457–487. https://doi.org/10.1210/EDRV.21.5.0410.

(5) Choe, S. S.; Huh, J. Y.; Hwang, I. J.; Kim, J. I.; Kim, J. B. Adipose Tissue Remodeling: Its Role in Energy Metabolism and Metabolic Disorders. Front Endocrinol (Lausanne) 2016, 7 (APR), 178543. https://doi.org/10.3389/FENDO.2016.00030/BIBTEX.

(6) Heller, I. J.; Nanda, R. Effect of Metabolic Alteration of Periodontal Fibers on Orthodontic Tooth Movement. An Experimental Study. Am J Orthod 1979, 75 (3), 239–258. https://doi.org/10.1016/0002-9416(79)90272-0.

(7) Cao, J. J. Effects of Obesity on Bone Metabolism. J Orthop Surg Res 2011, 6 (1), 1–7. https://doi.org/10.1186/1749-799X-6-30/FIGURES/1.

(8) Christenson, R. H. Biochemical Markers of Bone Metabolism: An Overview. Clin Biochem 1997, 30 (8), 573–593. https://doi.org/10.1016/S0009-9120(97)00113-6.

(9) Ozawa, H.; Hoshi, K.; Amizuka, N. Current Concepts of Bone Biomineralization. J Oral Biosci

2008, 50 (1), 1–14. https://doi.org/10.1016/S1349-0079(08)80014-X.

(10) Boskey, A. L. Biomineralization: An Overview. Connect Tissue Res 2003, 44 (SUPPL. 1), 5–9. https://doi.org/10.1080/03008200390152007.

(11) Cazalbou, S.; Combes, C.; Eichert, D.; Rey, C. Adaptative Physico-Chemistry of Bio-Related Calcium Phosphates. J Mater Chem 2004, 14 (14), 2148–2153. https://doi.org/10.1039/B401318B.

(12) Reznikov, N.; Shahar, R.; Weiner, S. Bone Hierarchical Structure in Three Dimensions. Acta Biomater 2014, 10 (9), 3815–3826. https://doi.org/10.1016/j.actbio.2014.05.024.

(13) Weiner, S.; Wagner, H. D. The Material Bone: Structure-Mechanical Function Relations. Annual Review of Materials Science 1998, 28 (1), 271–298. https://doi.org/10.1146/annurev.matsci.28.1.271.

(14) Rho, J. Y.; Kuhn-Spearing, L.; Zioupos, P. Mechanical Properties and the Hierarchical Structure of Bone. Med Eng Phys 1998, 20 (2), 92–102. https://doi.org/10.1016/S1350-4533(98)00007-1.

(15) Fantner, G. E.; Hassenkam, T.; Kindt, J. H.; Weaver, J. C.; Birkedal, H.; Pechenik, L.; Cutroni, J. A.; Cidade, G. A. G.; Stucky, G. D.; Morse, D. E.; Hansma, P. K. Sacrificial Bonds and Hidden Length Dissipate Energy as Mineralized Fibrils Separate during Bone Fracture. Nat Mater 2005, 4 (8), 612–616. https://doi.org/10.1038/nmat1428.

(16) Cavelier, S.; Dastjerdi, A. K.; McKee, M. D.; Barthelat, F. Bone Toughness at the Molecular Scale: A Model for Fracture Toughness Using Crosslinked Osteopontin on Synthetic and Biogenic Mineral Substrates. Bone 2018, 110, 304–311. https://doi.org/10.1016/j.bone.2018.02.022.

(17) Azzopardi, P. V.; O'Young, J.; Lajoie, G.; Karttunen, M.; Goldberg, H. A.; Hunter, G. K. Roles of Electrostatics and Conformation in Protein-Crystal Interactions. PLoS One 2010, 5 (2), 1–11. https://doi.org/10.1371/journal.pone.0009330.

(18) Fantner, G. E.; Adams, J.; Turner, P.; Thurner, P. J.; Fisher, L. W.; Hansma, P. K. Nanoscale Ion Mediated Networks in Bone: Osteopontin Can Repeatedly Dissipate Large Amounts of Energy. Nano Lett 2007, 7 (8), 2491–2498. https://doi.org/10.1021/nl0712769.

(19) Thompson, J. B.; Kindt, J. H.; Drake, B.; Hansma, H. G.; Morse, D. E.; Hansma, P. K. Bone Indentation Recovery Time Correlates with Bond Reforming Time. Nature 2001, 414 (6865), 773–776. https://doi.org/10.1038/414773a.

(20) Poundarik, A. A.; Diab, T.; Sroga, G. E.; Ural, A.; Boskey, A. L.; Gundberg, C. M.; Vashishth, D. Dilatational Band Formation in Bone. Proc Natl Acad Sci U S A 2012, 109 (47), 19178–19183. https://doi.org/10.1073/pnas.1201513109.

(21) Hunter, G. K.; OYoung, J.; Grohe, B.; Karttunen, M.; Goldberg, H. A. The Flexible Polyelectrolyte Hypothesis of Protein-Biomineral Interaction. Langmuir 2010, 26 (24), 18639–18646. https://doi.org/10.1021/la100401r.

(22) Hartmann, M. A.; Fratzl, P. Sacrificial Ionic Bonds Need to Be Randomly Distributed to Provide Shear Deformability. Nano Lett 2009, 9 (10), 3603–3607. https://doi.org/10.1021/nl901816s.

(23) Wang, Y.; Morsali, R.; Dai, Z.; Minary-Jolandan, M.; Qian, D. Computational Nanomechanics of Noncollagenous Interfibrillar Interface in Bone. ACS Appl Mater Interfaces 2020, 12 (22), 25363–25373. https://doi.org/10.1021/acsami.0c01613.

(24) Currey, J. Sacrificial Bonds Heal Bone. Nature 2001, 414 (6865), 699. https://doi.org/10.1038/414699a.

(25) Nurminskaya, M.; Kaartinen, M. T. Transglutaminases in Mineralized Tissues. Frontiers in Bioscience 2006, 11 (2 P.1591-2006), 1591–1606. https://doi.org/10.2741/1907/PDF.

(26) Gaharwar, A. K.; Dammu, S. A.; Canter, J. M.; Wu, C. J.; Schmidt, G. Highly Extensible, Tough, and Elastomeric Nanocomposite Hydrogels from Poly(Ethylene Glycol) and Hydroxyapatite Nanoparticles. Biomacromolecules 2011, 12 (5), 1641–1650. https://doi.org/10.1021/bm200027z.

(27) Podsiadlo, P.; Kaushik, A. K.; Arruda, E. M.; Waas, A. M.; Shim, B. S.; Xu, J.; Nandivada, H.; Pumplin, B. G.; Lahann, J.; Ramamoorthy, A.; Kotov, N. A. Ultrastrong and Stiff Layered Polymer Nanocomposites. Science (1979) 2007, 318 (5847), 80–83. https://doi.org/10.1126/science.1143176.

(28) Liu, R.; Liang, S.; Tang, X. Z.; Yan, D.; Li, X.; Yu, Z. Z. Tough and Highly Stretchable Graphene Oxide/Polyacrylamide Nanocomposite Hydrogels. J Mater Chem 2012, 22 (28), 14160–14167. https://doi.org/10.1039/c2jm32541a.

(29) Haraguchi, K. Nanocomposite Gels: New Advanced Functional Soft Materials. Macromol Symp 2007, 256, 120–130. https://doi.org/10.1002/masy.200751014.

(30) Sun, T. L.; Kurokawa, T.; Kuroda, S.; Ihsan, A. Bin; Akasaki, T.; Sato, K.; Haque, M. A.; Nakajima, T.; Gong, J. P. Physical Hydrogels Composed of Polyampholytes Demonstrate High Toughness and Viscoelasticity. Nat Mater 2013, 12 (10), 932–937. https://doi.org/10.1038/nmat3713.

(31) Luo, F.; Sun, T. L.; Nakajima, T.; King, D. R.; Kurokawa, T.; Zhao, Y.; Ihsan, A. Bin; Li, X.; Guo, H.; Gong, J. P. Strong and Tough Polyion-Complex Hydrogels from Oppositely Charged Polyelectrolytes: A Comparative Study with Polyampholyte Hydrogels. Macromolecules 2016, 49 (7), 2750–2760. https://doi.org/10.1021/acs.macromol.6b00235.

(32) Perrin, F. X.; Nguyen, V.; Vernet, J. L. FT-IR Spectroscopy of Acid-Modified Titanium Alkoxides: Investigations on the Nature of Carboxylate Coordination and Degree of Complexation. J Solgel Sci Technol 2003, 28 (2), 205–215. https://doi.org/10.1023/A:1026081100860.

(33) Fantner, G. E.; Oroudjev, E.; Schitter, G.; Golde, L. S.; Thurner, P.; Finch, M. M.; Turner, P.; Gutsmann, T.; Morse, D. E.; Hansma, H.; Hansma, P. K. Sacrificial Bonds and Hidden Length: Unraveling Molecular Mesostructures in Tough Materials. Biophys J 2006, 90 (4), 1411–1418. https://doi.org/10.1529/biophysj.105.069344.

(34) Takahashi, R.; Sun, T. L.; Saruwatari, Y.; Kurokawa, T.; King, D. R.; Gong, J. P. Creating Stiff, Tough, and Functional Hydrogel Composites with Low-Melting-Point Alloys. Advanced Materials 2018, 30 (16), 1–7. https://doi.org/10.1002/adma.201706885.

(35) Gong, J. P. Materials Both Tough and Soft. Science (1979) 2014, 344 (6180), 161–162. https://doi.org/10.1126/science.1252389.

(36) Matsuda, T.; Nakajima, T.; Gong, J. P. Fabrication of Tough and Stretchable Hybrid Double-Network Elastomers Using Ionic Dissociation of Polyelectrolyte in Nonaqueous Media. Chemistry of Materials 2019, 31 (10), 3766–3776. https://doi.org/10.1021/acs.chemmater.9b00871.

(37) Ducrot, E.; Chen, Y.; Bulters, M.; Sijbesma, R. P.; Creton, C. Toughening Elastomers with

Sacrificial Bonds and Watching Them Break. Science (1979) 2014, 344 (6180), 186–189. https://doi.org/10.1126/science.1248494.

(38) Zhou, X.; Guo, B.; Zhang, L.; Hu, G. H. Progress in Bio-Inspired Sacrificial Bonds in Artificial Polymeric Materials. Chem Soc Rev 2017, 46 (20), 6301–6329. https://doi.org/10.1039/c7cs00276a.

(39) Haque, M. A.; Kurokawa, T.; Kamita, G.; Gong, J. P. Lamellar Bilayers as Reversible Sacrificial Bonds to Toughen Hydrogel: Hysteresis, Self-Recovery, Fatigue Resistance, and Crack Blunting. Macromolecules 2011, 44 (22), 8916–8924. https://doi.org/10.1021/ma201653t.

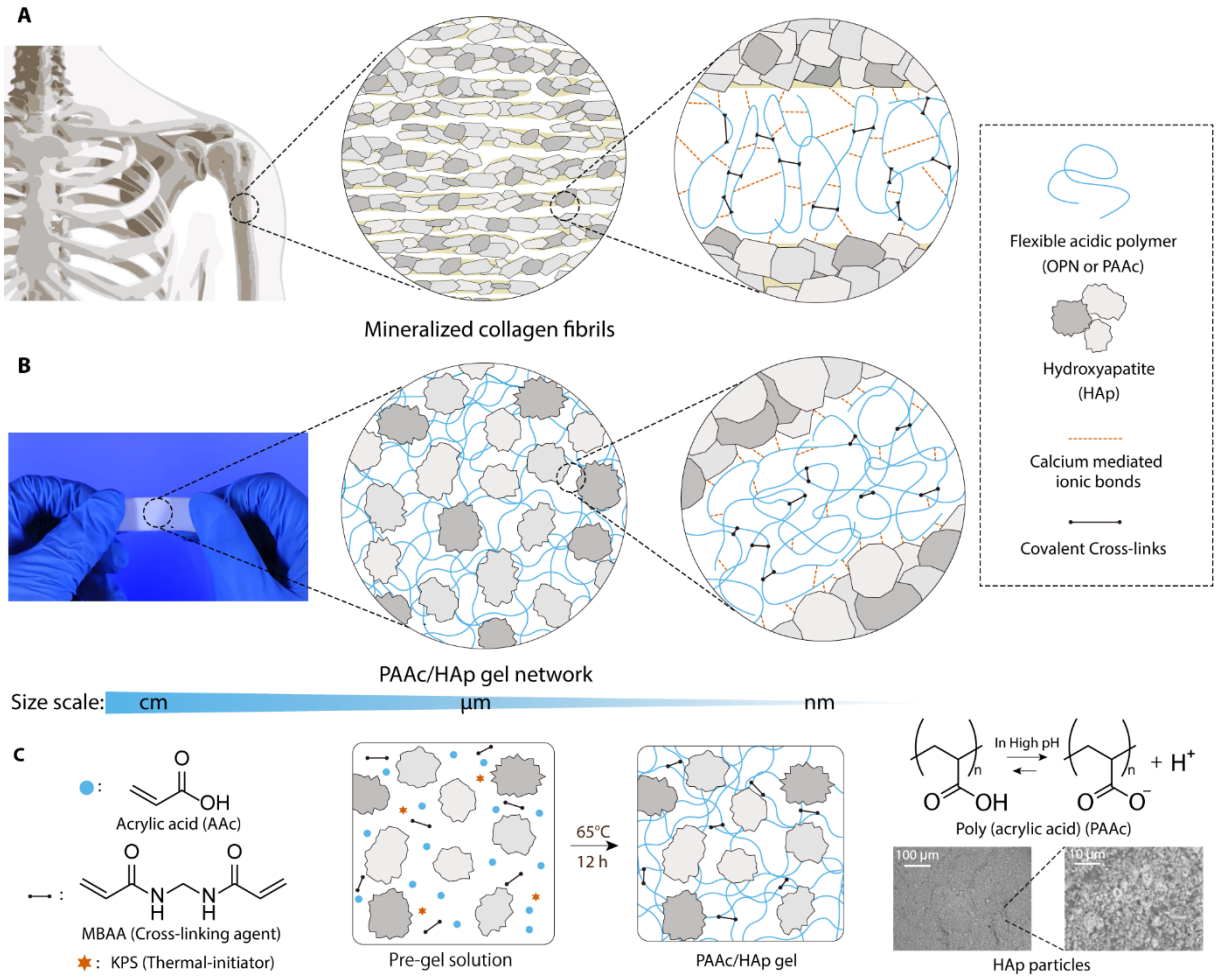

Figure 3-1. Schematic representation of A) bone with sacrificial bonding structures at molecular level and B) PAAc/HAp hydrogel with sacrificial bonds formed by bone-like self-regulative mechanism. C) Synthesis protocol of PAAc/HAp hydrogels. Inset scanning electron microscope (SEM) image was HAp raw particles.

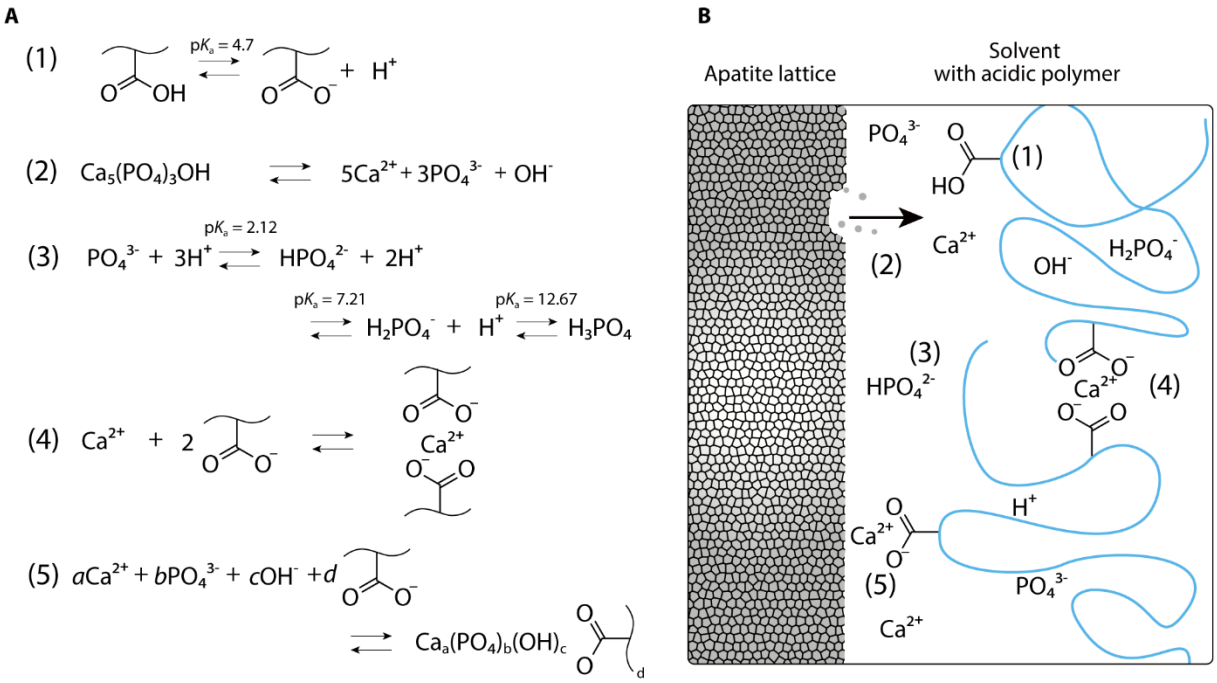

Figure 3-2. A) Five coupled equilibrium reactions of acidic polymers PAAc and HAp in self-regulation of sacrificial bonds to form tough hydrogels and B) their schematic diagram.

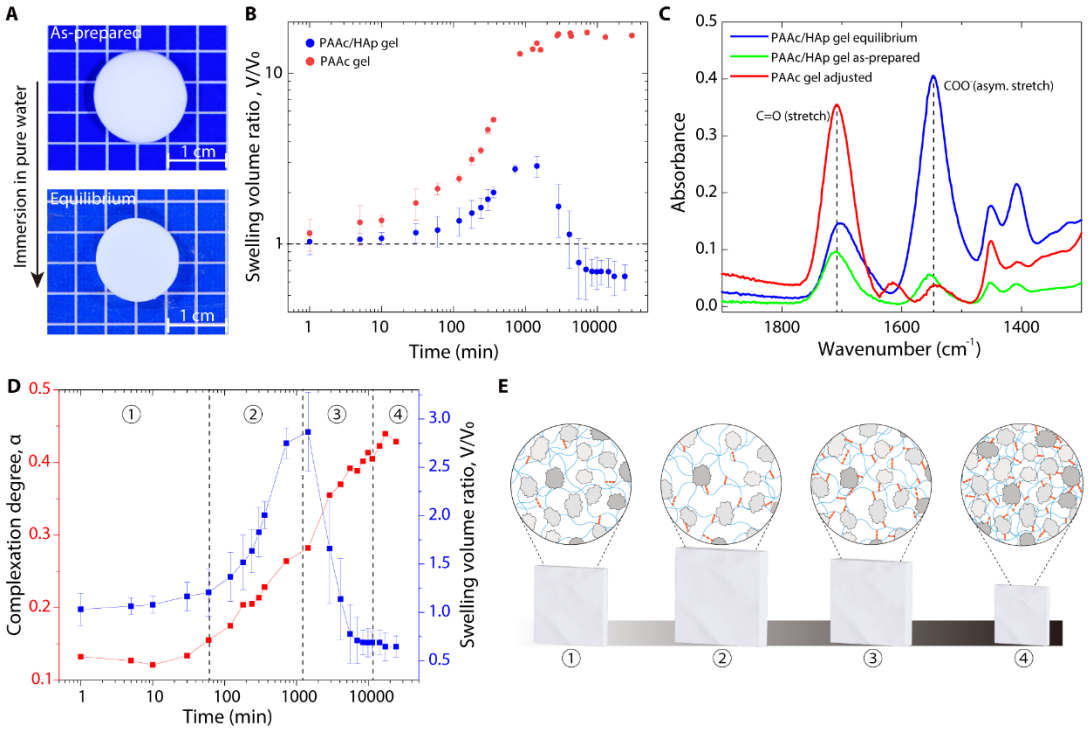

Figure 3-3. A) Appearances of the as-prepared PAAc/HAp gel and its equilibrated one in pure water. B) Chronological change in swelling volume ratio of PAAc/HAp gel and PAAc gel when immersed in pure water. C) ATR-FTIR spectra of as-prepared and equilibrium PAAc/HAp gels, and of PAAc gel adjusted to the same volume of the equilibrated PAAc/HAp gel. D) Complexation degree calculated from FTIR spectra and swelling volume ratio change over time. E) Schematic depiction of swelling and deswelling behavior of PAAc/HAp gel. The inset numbers are corresponding to those in Figure 4D. The PAAc/HAp gel of formulation 3 M AAc, 0.1 mol% MBAA, and 10 vol% HAp was used as a typical example.

Table 3-1. Ion concentrations produced by coupled equilibrium reactions for a sample prepared with a formulation of 3M AAc, 0.1 mol % MBAA, 10 vol % HAp. The results with *, †, and ‡ are experimental values determined by IR (*), ICP (†), and TG-DTA (‡) and others are calculated values based on mass conservation law. All concentrations are relative to volume of the as-prepared gel. The concentrations of H^+, PO_4^{3-}, and OH^- in the equilibrated PAAc/HAp gel are assumed zero for simplicity.

		PAAc		**HAp**			**PAAc/HAp**
In feed		AAc 3 M		$Ca_5(PO_4)_3(OH)$ (10 vol%) 0.6 M (Ca: 3 M, P 1.8 M, OH, 0.6 M)			0.68 ‡ (wt/wt)
Equilibrated	Ions dissolved from HAp	-	-	Ca^{2+} 1.11 M (37%)	PO_4^{3-} 0.67 M (37%)	OH^- 0.22 M (37%)	0.72 ‡ (wt/wt)
	Ions	**H^+**	**$RCOO^-$**	**Ca^{2+}**	**PO_4^{3-}**	**OH^-**	**+/- charge ratio**
	In gel	0 M	1.68 M* α=0.56	0.78 M (26%)	0 M	0M	~1
	In solution	1.68 M α=0.56	0 M	0.33 M † (11%)	0.67 M † (37%)	0.22 M (37%)	~1

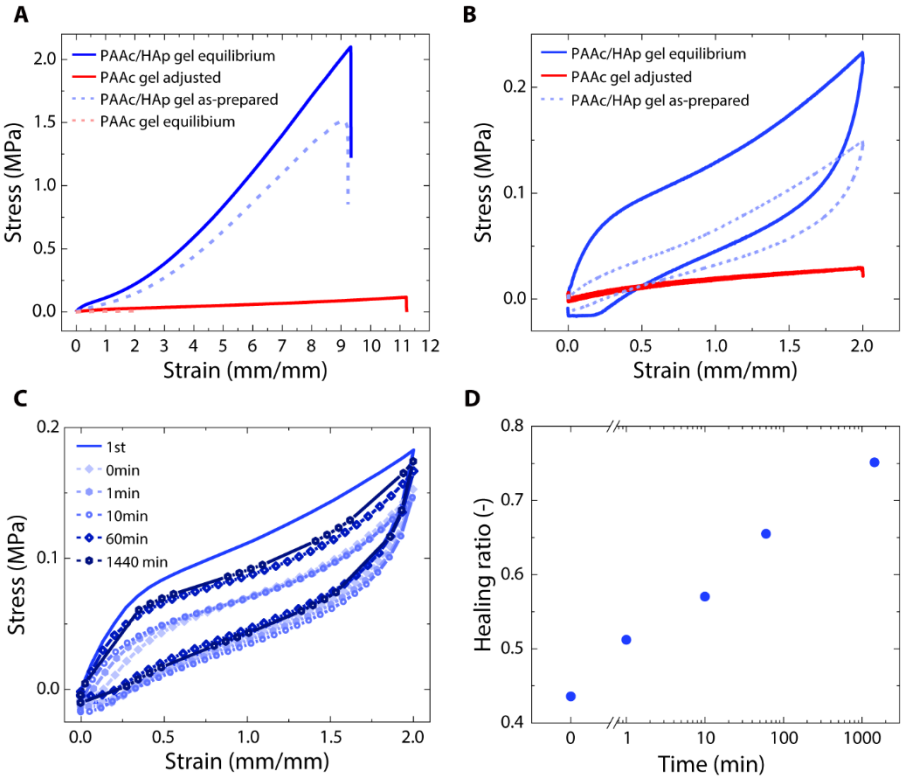

Figure 3-4. A) Tensile stress-strain curves of as-prepared and equilibrated PAAc/HAp gels, equilibrated PAAc gel and swelling-adjusted PAAc gel. B) Cyclic loading/unloading tests of as-prepared PAAc/HAp gel, equilibrated PAAc/HAp gel and adjusted PAAc gel. C) Cyclic loading/unloading tests to evaluate healing ratio of equilibrated PAAc/HAp gel with different waiting times after the 1st cycle. D) Healing ratio calculated from the hysteresis in C. The PAAc/HAp gel of formulation 3 M AAc, 0.1 mol% MBAA, and 10 vol% HAp was used.

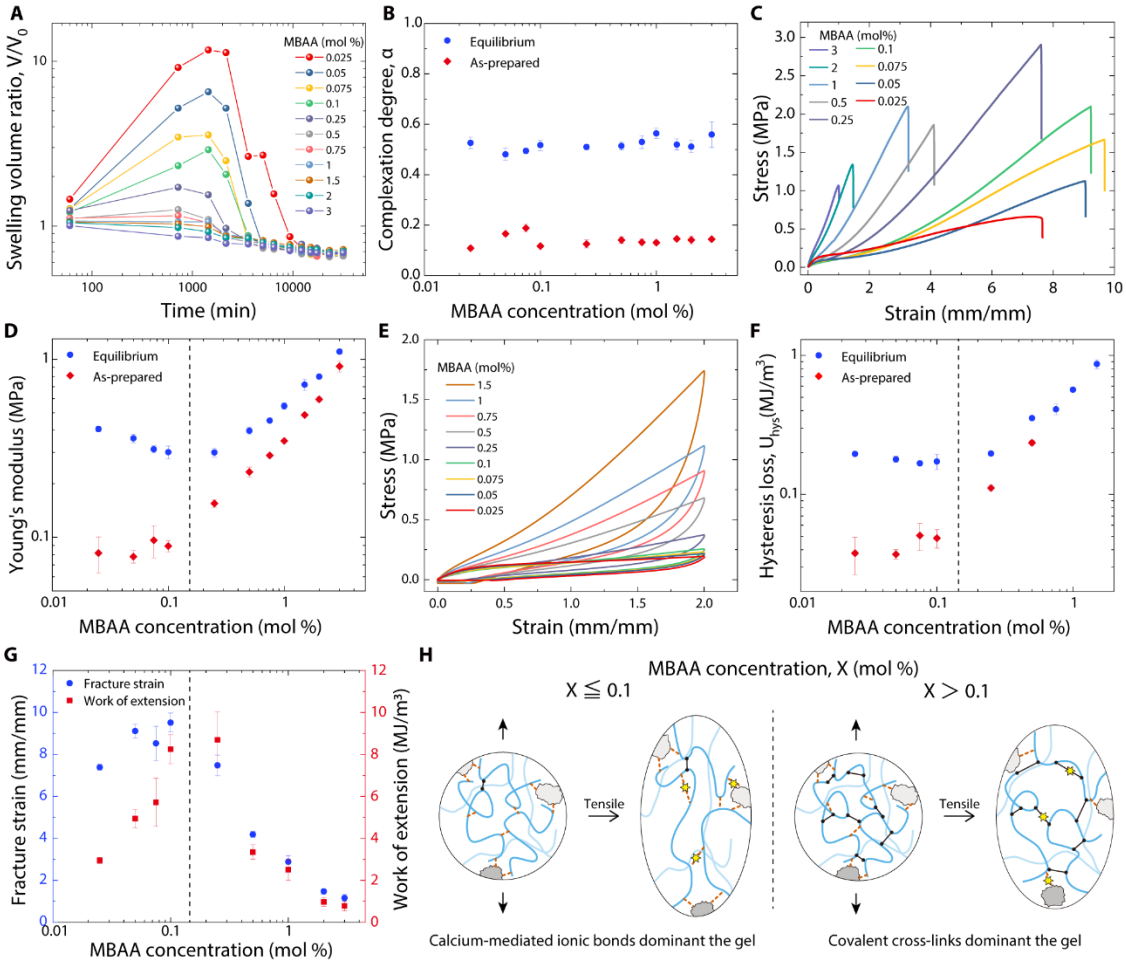

Figure 3-5. Various physical properties of PAAc/HAp gels with varying cross-linker (MBAA) concentrations from 0.025 to 3 mol%, and the AAc (3 M) and HAp (10 vol%) were kept constant. A) Swelling volume ratio, B) Complexation degree, C) Tensile stress strain curves, D) Young's modulus, E) Cyclic loading/unloading curves, F) Hysteresis loss calculated from E, G) Fracture strain and Work of extension. The dash lines in D, F and G means the transition boundary between the ionic cross-linking dominant and covalent cross-link dominant. H) Schematic images of the PAAc/HAp cross-linked network in varying MBAA concentrations. Left one is the ionic cross-link dominant network below 0.1 mol% MBAA concentrations and the right one is the covalent cross-link dominant network above 0.1 mol%.

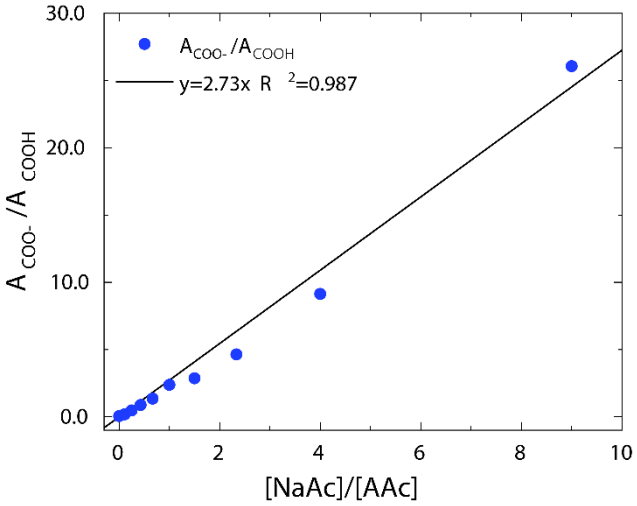

Figure 3-S1. FT-IR spectra peak ratios at 1550 cm^{-1} (assigned to COO-) and 1700 cm^{-1} (assigned to COOH) of poly(NaAc-co-AAc) gels synthesized from copolymerization of sodium salt acrylic acid monomer (NaAc) and acrylic acid monomer (AAc) of different ratios [NaAc]/[AAc] with a total monomer concentration 1 M. The curve was used as the calibration curve to determine the complexation degree α in PAAc/HAp and PAAc gels from the FT-IR spectra, assuming that the measured peak area ratio A_{COO-}/A_{COOH} equals to the dissociation ratio of carboxyl groups.

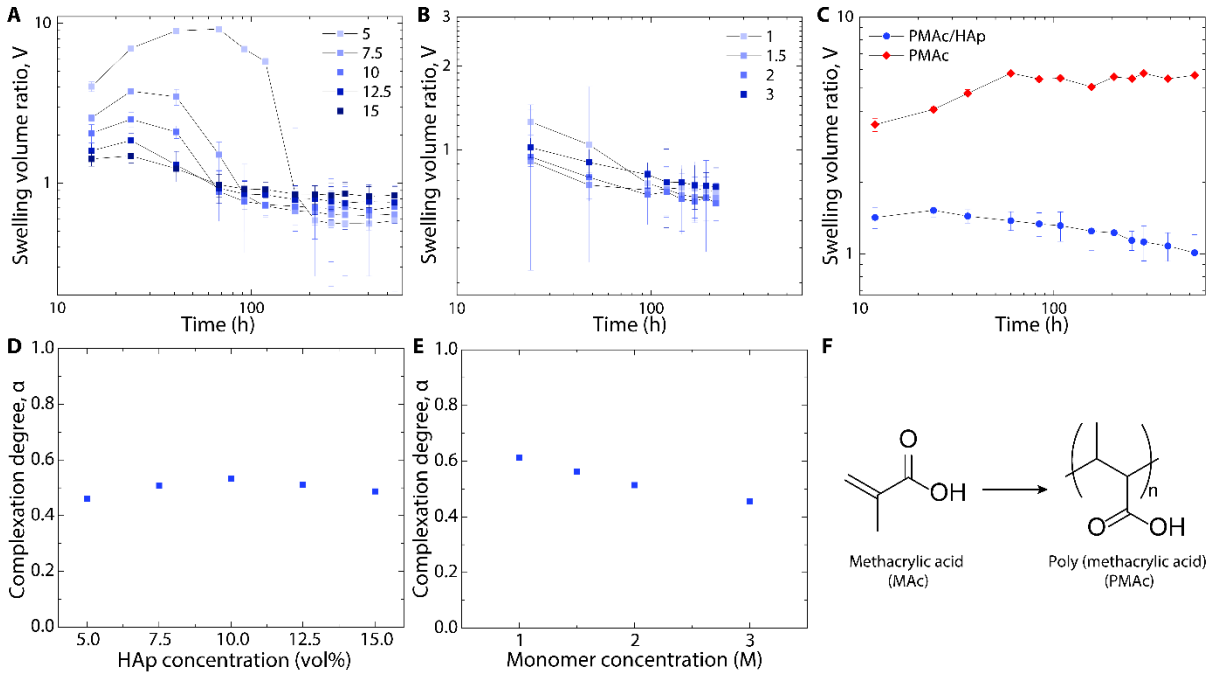

Figure 3-S2. A) Chronological change in swelling volume ratio of PAAc/HAp gel prepared with various HAp concentration (AAc 3 M, MBAA 0.1 mol%) when immersed in pure water. B) Chronological change in swelling volume ratio of PAAc/HAp gel prepared with various AAc concentration (MBAA 1 mol%, HAp 10 vol%) when immersed in pure water. C) Chronological change in swelling volume ratio of PMAc/HAp gel (MAc 3 M, MBAA 0.1 mol%, HAp 10 vol%) and the corresponding PMAc gel when immersed in pure water. D) Complexation degree of equilibrated PAAc/HAp gel with various HAp concentration calculated from FTIR spectra. E) Complexation degree of equilibrated PAAc/HAp gel with various PAAc concentration calculated from FTIR spectra.

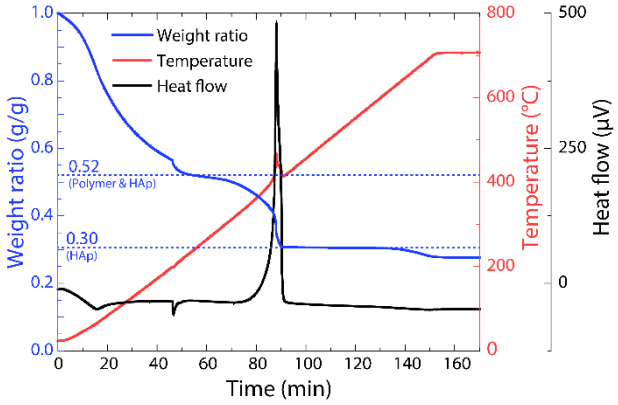

Figure 3-S3. TG-DTA profile to calculate fractions of polymers and HAp of PAAc/HAp gel. Sharp endothermic peak at 200 °C indicates evaporation of hydrated layer.

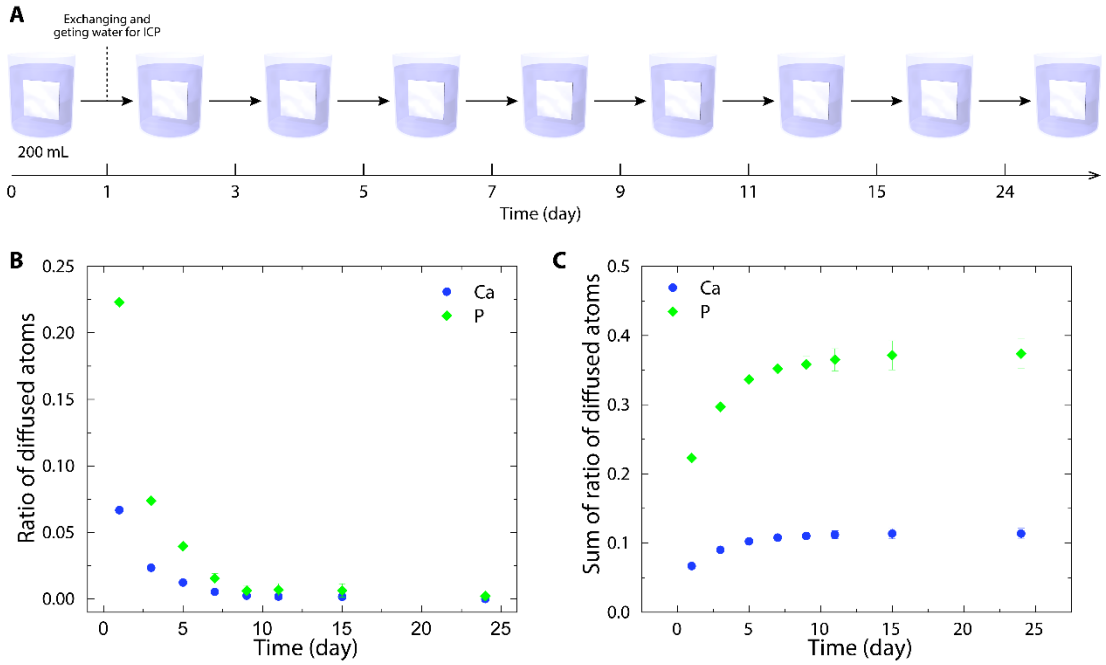

Figure 3-S4. Results of ICP analysis. A) Schematic illustration of experimental procedure. B) chronological change of ratio of diffused ions from feed HAp particles. C) Sum of the ratio of diffused ions. The ratio is in relative to the initial total amount of each component.

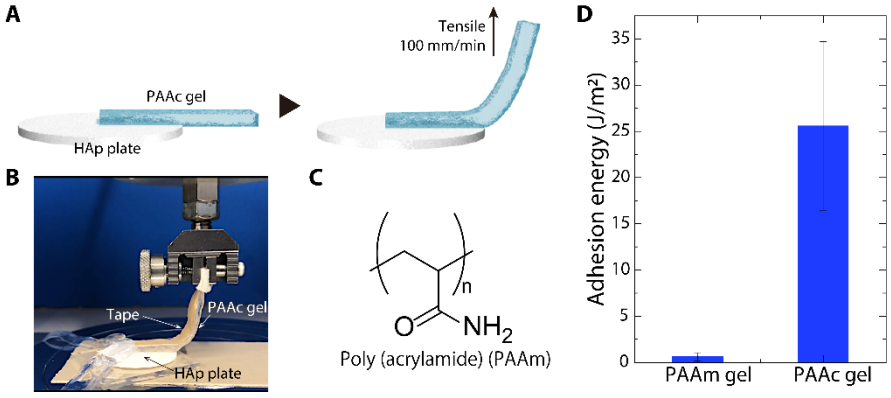

Figure 3-S5. Peeling test of PAAc gel on HAp plate. A) Schematic illustration of the peeling test. B) Photo of the peeling test. C) Formula of non-acidic polymer for the control test. D) Adhesion energy of the gels to HAp plate from the peeling test.

Acknowledgement

This research on this dissertation has been carried out in the Laboratory of Soft and Wet matter (LSW), Graduate School of Life Science, Hokkaido University, Japan, supervised by Professor Jian Ping Gong. Associate examiners are Professor Kuniharu Ijiro, Associate Professor Li Xiang, Associate Professor Takayuki Nonoyama, Associate professor Tasuku Nakajima and Associate Professor Tsutomu Indei.

First of all, I am extremely grateful for the support and encouragement of my esteemed advisors, Professor Jian Ping Gong and Associate Professor Takayuki Nonoyama. They have given me not only scientific support but also support regarding my life and mental health. Without them, I definitely could not have carried out my PhD program.

I would like to thank also to Associate Professor Tasuku Nakajima, Associate Professor Tsutomu Indei and Associate Professor Li Xiang. I learned a lot from the many scientific discussions with them.

As well as the supervisors, I am grateful to Ms. Yuki Suzuki, Mr. Kazuki Tanaka, Dr. Kazuki Fukao and Dr. Ryuji Kiyama who were the senior students and the good advisors for my research. I was able to learn what research is all about by watching their backs.

I want to gratefully acknowledge Hokkaido University's "DX doctoral fellowship" supported by JST, Japan supporting my research. It was impossible to complete my doctoral research without their financial support.

Finally, special thanks to my father, my mother, my sister and my sweet cats, Momen and Kinu, for their support and encouragement. This dissertation is dedicated to them.

Naohiro Kashimura

Laboratory of Soft & Wet Matter
Graduate School of Life Science
Hokkaido University
Sapporo Japan
June 2024

Tough Hydroxyapatite Hydrogels Based on Bone-like Self-Regulatory Sacrificial Bond Formation

Author: Naohiro Kashimura, Yuki Suzuki, Takayuki Nonoyama, et al

Publication: Chemistry of Materials

Publisher: American Chemical Society

Date: Mar 1, 2024

PERMISSION/LICENSE IS GRANTED FOR YOUR ORDER AT NO CHARGE

This type of permission/license, instead of the standard Terms and Conditions, is sent to you because no fee is being charged for your order. Please note the following:

- Permission is granted for your request in both print and electronic formats, and translations.
- If figures and/or tables were requested, they may be adapted or used in part.
- Please print this page for your records and send a copy of it to your publisher/graduate school.
- Appropriate credit for the requested material should be given as follows: "Reprinted (adapted) with permission from {COMPLETE REFERENCE CITATION}. Copyright {YEAR} American Chemical Society." Insert appropriate information in place of the capitalized words.
- One-time permission is granted only for the use specified in your RightsLink request. No additional uses are granted (such as derivative works or other editions). For any uses, please submit a new request.

If credit is given to another source for the material you requested from RightsLink, permission must be obtained from that source.

BACK CLOSE WINDOW